

A-17

NACA TN 2417

# NATIONAL ADVISORY COMMITTEE FOR AERONAUTICS

TECHNICAL NOTE 2417 ✓

## PRELIMINARY STUDY OF STABILITY OF FLOW FROM TWO DUCTS DISCHARGING INTO A COMMON DUCT

By Albert I. Bellin, D. Richard Messina  
and Paul B. Richards

Harvard University



Washington  
July 1951

NATIONAL ADVISORY COMMITTEE FOR AERONAUTICS

---

TECHNICAL NOTE 2417

---

## PRELIMINARY STUDY OF STABILITY OF FLOW FROM TWO DUCTS

## DISCHARGING INTO A COMMON DUCT

By Albert I. Bellin, D. Richard Messina  
and Paul B. Richards

## SUMMARY

This research is a preliminary investigation of the instability of flow from two ducts that join into a common duct and of the influence of the various parameters upon the phenomenon.

A two-dimensional potential analysis was carried out under the assumption that the two ducts discharge into a region of constant pressure. For this problem, there exists a unique solution if a Joukowski hypothesis is imposed; also, the results indicate the flow to be stable with respect to small changes in the physical parameters. This is confirmed by experiments with a two-dimensional water table. The simplified model, therefore, does not explain oscillations and asymmetries of flow for actual symmetric duct configurations.

The problem is reconsidered with the assumption of turbulent mixing between the jet from the two ducts and the surrounding fluid in the common duct. On this basis, qualitative considerations indicate that self-excited forces may arise to account for observed instabilities.

Experiments with a two-dimensional water table indicate three different flow régimes for a symmetric system of two ducts that converge and discharge into an expanded duct (or sink):

(1) For a ratio of sink width to duct width of about 55, the jet leaving the two ducts oscillates about the symmetry axis. Under certain conditions, the oscillations are periodic.

(2) For a ratio of sink width to duct width of about 35, there are three flows possible. Two are steady with the jet asymmetric; the third is periodic with the jet moving laterally about the symmetry axis.

(3) For a ratio of sink width to duct width of about 20, the flow is steady with the jet asymmetric to the right or left.

In the last two cases, sufficiently large external disturbances shift the flow from one pattern to another. The periodic oscillations of the jet have a frequency of the order of 0.30 cycle per second and an amplitude of 5° to 10°.

### INTRODUCTION

This report is concerned with a theoretical and experimental investigation of oscillations and asymmetries in the flow from two ducts discharging into a common duct.

Dimensional considerations show that, if there is an oscillation in a fluid-flow problem, the frequency  $f$  is given by

$$f = \frac{V}{l} F(R, M)$$

where

$V$  characteristic velocity of flow

$l$  characteristic length

$R$  Reynolds number  $\left(\frac{Vl}{\nu}\right)$

$\nu$  kinematic viscosity

$M$  Mach number  $\left(\frac{V}{a}\right)$

$a$  characteristic acoustic velocity of flow

The above functional form for  $f$  considers the effects of scale, inertia, viscosity, and compressibility. If turbulent effects are to be pertinent in the problem, and if the mixing-length theory is taken as a simple model for turbulence, a new dimensionless quantity  $c$  should be introduced as one of the variables. The quantity  $c$ , which is the ratio between the so-called mixing length and a characteristic length variable, is usually taken to be a constant independent of fluid. Thus,  $f$  has the same form if turbulence is important in the problem.

In some instances, such as the case of acoustic oscillations in a simple duct system, the effect of  $R$  upon frequency is relatively unimportant. Here, if  $V$  is the fluid velocity in the duct,

$$f = K \frac{a}{L} (1 - M^2)$$

where

- K constant determined by geometry of system and mode  
L characteristic duct length

For other problems, the Reynolds number is the determining variable for the oscillation. An example of this occurs in pipe flow with a Reynolds number in the critical region where the flow pulsates periodically between a laminar and a turbulent state.

In the particular case of flow from two ducts discharging into a common duct, oscillations, or surging of the fluid alternately in the two ducts, as well as asymmetry in the flow for a symmetric setup have been observed. The oscillations have been of relatively low frequency, large amplitude, and, in some cases, of a destructive nature. This suggests viscosity or turbulence rather than compressibility as the cause of the phenomenon. Since compressible effects have been ruled out, for experimental convenience water, rather than air, has been used for the most part as the fluid.

The purpose of the experiments was to try to duplicate and to observe the undesirable oscillations and instabilities and to determine the effects of the various parameters. A potential solution that approximates the physical picture was examined analytically to determine the form of the ideal flow and to see if the theoretical solution is unique. It should be noted that for the related problem of two impinging free streams the potential solution is not unique; evidently in this case a stability condition is necessary to specify the "correct" solution. (See reference 1.) Also, in a qualitative way, the phenomenon has been considered in the light of turbulent mixing effects.

#### THEORETICAL ANALYSIS

The physical problem that is to be idealized is that of the flow from two ducts that join and discharge into a single expanded duct as shown in figure 1. Unless the velocity is extremely low, the flow

enters the fluid in the large duct as a jet. A reasonable and simple approximation to this physical model is to consider the two-dimensional potential flow out of two straight joined ducts into an atmosphere of uniform pressure (see fig. 2(a)).

For the present, it is assumed that both streams come from one reservoir and so have the same density and the same stagnation pressure. The ducts meet at an angle  $\beta$  and have cross-sectional areas  $A_1$  and  $A_2$ . Infinitely far back inside the ducts at points A and B the fluid-velocity magnitudes are  $q_1$  and  $q_2$ , respectively. The free streamlines DF and EF have a velocity magnitude  $q_a$ . At infinity in the free stream, point F, the flow makes an angle  $\gamma$  with the x-axis. Point C, which is common to both ducts, must be a stagnation point if there are to be no infinite velocities in the flow field.

The  $w'$  plane, or the hodograph plane defined by

$$w' = u - iv$$

is shown in figure 2(b) where  $u$  and  $v$  are the  $x$  and  $y$  components of velocity. It is seen that the flow fills a sector of a circle in the  $w'$  plane. The transformation

$$\zeta = (w')^{\pi/\beta}$$

where  $\beta$  is the angle between the ducts, expands the sector into a semicircle (fig. 3(a)). Then the transformation

$$\eta = \zeta + \frac{q_a^{2\pi/\beta}}{\zeta}$$

maps the semicircle in the  $\zeta$ -plane into the upper half of the  $\eta$ -plane (fig. 3(b)). The complex potential  $w$ , defined by

$$w = \phi + i\psi$$

where  $\phi$  and  $\psi$  are the potential and stream functions, respectively, is given by the superposition of a source at  $\eta_a$ , a source at  $\eta_b$ , and a sink at  $\eta_f$ :

$$w = \frac{A_1 q_1}{\pi} \log_e \frac{\eta - \eta_a}{\eta - \eta_f} + \frac{A_2 q_2}{\pi} \log_e \frac{-\eta + \eta_b}{\eta - \eta_f}$$

The statement that  $C$  is a stagnation point requires that  $\frac{dw}{d\eta} = 0$  for  $\eta = \infty$  since  $C$  is mapped into infinity in the  $\eta$ -plane. This condition yields the relation

$$\eta_f = \frac{A_1 q_1 \eta_a + A_2 q_2 \eta_b}{A_1 q_1 + A_2 q_2}$$

For convenience, the following symbols are introduced:

$$\frac{q_1}{q_a} = s_1$$

$$\frac{q_2}{q_a} = s_2$$

$$s_1^{\pi/\beta} + s_1^{-\pi/\beta} = 2\sigma_1$$

$$s_2^{\pi/\beta} + s_2^{-\pi/\beta} = 2\sigma_2$$

$$\frac{A_1}{A_2} = \alpha$$

In the new notation,

$$\eta_a = 2q_a^{\pi/\beta} \sigma_1$$

$$-\eta_b = 2q_a^{\pi/\beta} \sigma_2$$

$$w_f' = q_a e^{-i\gamma}$$

$$\zeta_f = q_a \frac{\pi/\beta}{e^{-i\pi\gamma/\beta}}$$

$$\eta_f = 2q_a \frac{\pi/\beta}{\cos \frac{\pi\gamma}{\beta}}$$

and the relation for  $\eta_f$  may be rewritten to give

$$\cos \frac{\pi\gamma}{\beta} = \frac{\alpha S_1 \sigma_1 - S_2 \sigma_2}{\alpha S_1 + S_2}$$

This last equation relates the angle  $\gamma$  of the free stream at infinity with the area ratio  $\alpha$ , the dimensionless speeds  $S_1$  and  $S_2$ , and the angle of convergence  $\beta$  of the ducts.

To complete the solution, the detailed flow should be expressed in terms of the geometry in the physical plane. Only the functions  $S_1$ ,  $S_2$ , and  $\gamma$  shall be given here. To specify the problem, the distances  $X$  and  $Y$  in addition to  $A_1$ ,  $A_2$ , and the angle  $\beta$  (see fig. 4) must be known. First, it is convenient to introduce the distances  $\delta$  and  $\Delta$ .

Along a free streamline,

$$dw = d\phi = q_a ds$$

$$w' = q_a e^{-i\theta}$$

$$\zeta = q_a \frac{\pi/\beta}{e^{-i\pi\theta/\beta}}$$

$$\eta = 2q_a \frac{\pi/\beta}{\cos \frac{\pi\theta}{\beta}}$$

$$d\eta = -2 \frac{\pi}{\beta} q_a \frac{\pi/\beta}{\sin \frac{\pi\theta}{\beta}} d\theta$$

or

$$\frac{dw}{d\eta} = \frac{-q_a}{2 \frac{\pi}{\beta} q_a \frac{\pi/\beta}{\sin \frac{\pi\theta}{\beta}}} \frac{ds}{d\theta}$$

where  $ds$  is distance along the free streamline and  $\theta$  is the angle that the velocity vector makes with the  $x$ -direction. By direct differentiation of the complex potential, however,

$$\frac{dw}{d\eta} = \frac{A_1 q_1}{\pi} \left( \frac{1}{\eta - \eta_a} - \frac{1}{\eta - \eta_f} \right) + \frac{A_2 q_2}{\pi} \left( \frac{1}{\eta - \eta_b} - \frac{1}{\eta - \eta_f} \right)$$

Equating the two values  $\frac{dw}{d\eta}$  and solving for  $\frac{ds}{d\theta}$ ,

$$\frac{ds}{d\theta} = - \frac{2}{\beta} q_a^{\frac{\pi}{2}-1} \sin \frac{\pi\theta}{\beta} \left[ A_1 q_1 \left( \frac{1}{\eta - \eta_a} - \frac{1}{\eta - \eta_f} \right) + A_2 q_2 \left( \frac{1}{\eta - \eta_b} - \frac{1}{\eta - \eta_f} \right) \right]$$

The quantity  $h$  is now given by

$$h = \int_{\beta}^{\gamma} \frac{ds}{d\theta} \sin(\theta - \gamma) d\theta - \int_0^{\gamma} \frac{ds}{d\theta} \sin(\theta - \gamma) ds$$

where  $\Delta = h + A_a$  and  $A_a$  is the cross-sectional area of the jet at infinity and is equal to  $S_1 A_1 + S_2 A_2$ . Also, the distance  $\delta$  can now be written

$$\delta = \int_0^{\gamma} \frac{ds}{d\theta} \cos(\theta - \gamma) d\theta + \int_{\gamma}^{\beta} \frac{ds}{d\theta} \cos(\theta - \gamma) d\theta$$

Then X and Y are given by

$$X = (\delta + \Delta \cot \beta) \cos \gamma + (\Delta - \delta \cot \beta) \sin \gamma$$

$$Y = \csc \beta (\Delta \cos \gamma - \delta \sin \gamma)$$

To point out the essential features of the flow, the solution is included for a specific value of the duct convergence angle:

$$\beta = \frac{\pi}{2}$$

For this special case,

$$\begin{aligned} \frac{h}{A_2} = & -\frac{2}{\pi} \cos \gamma \left[ \alpha S_1 \left( 1 - \sqrt{\frac{\sigma_1 - 1}{2}} \tan^{-1} \sqrt{\frac{2}{\sigma_1 - 1}} \right) + \right. \\ & S_2 \left( 1 - \sqrt{\frac{\sigma_2 + 1}{2}} \tanh^{-1} \sqrt{\frac{2}{\sigma_2 + 1}} \right) - \\ & \left. \frac{2}{\pi} \sin \gamma \left[ \alpha S_1 \left( 1 - \sqrt{\frac{\sigma_1 + 1}{2}} \tanh^{-1} \sqrt{\frac{2}{\sigma_1 + 1}} \right) + \right. \right. \\ & S_2 \left( 1 - \sqrt{\frac{\sigma_2 - 1}{2}} \tan^{-1} \sqrt{\frac{2}{\sigma_2 - 1}} \right) + \frac{2}{\pi} (\alpha S_1 + S_2) (\cos \gamma + \sin \gamma) + \\ & \left. \frac{1}{\pi} (\alpha S_1 + S_2) \sin \gamma \cos \gamma \log_e \frac{(1 - \sin \gamma)(1 - \cos \gamma)}{(1 + \sin \gamma)(1 + \cos \gamma)} \right] \end{aligned}$$

$$\begin{aligned}
 \frac{\delta}{A_2} = & \frac{2}{\pi} \sin \gamma \left[ \alpha S_1 \left( 1 - \sqrt{\frac{\sigma_1 - 1}{2}} \tan^{-1} \sqrt{\frac{2}{\sigma_1 - 1}} \right) + \right. \\
 & S_2 \left( 1 - \sqrt{\frac{\sigma_2 + 1}{2}} \tanh^{-1} \sqrt{\frac{2}{\sigma_2 + 1}} \right) - \\
 & \left. \frac{2}{\pi} \cos \gamma \left[ \alpha S_1 \left( 1 - \sqrt{\frac{\sigma_1 + 1}{2}} \tanh^{-1} \sqrt{\frac{2}{\sigma_1 + 1}} \right) + \right. \right. \\
 & S_2 \left( 1 - \sqrt{\frac{\sigma_2 - 1}{2}} \tan^{-1} \sqrt{\frac{2}{\sigma_2 - 1}} \right) - \frac{2}{\pi} (\alpha S_1 + S_2) (\sin \gamma - \cos \gamma) - \\
 & \left. \left. \frac{1}{\pi} (\alpha S_1 + S_2) \log_e \left[ \frac{(1 - \sin \gamma)(1 + \cos \gamma)}{(1 + \sin \gamma)(1 - \cos \gamma)} \right] \right]
 \end{aligned}$$

$$\begin{aligned}
 \frac{x}{A_2} = & \frac{2\alpha S_1}{\pi} \sqrt{\frac{\sigma_1 + 1}{2}} \tanh^{-1} \sqrt{\frac{2}{\sigma_1 + 1}} + \frac{2S_2}{\pi} \sqrt{\frac{\sigma_2 - 1}{2}} \tan^{-1} \sqrt{\frac{2}{\sigma_2 - 1}} + \\
 & (\alpha S_1 + S_2) \sin \gamma - \frac{1}{\pi} (\alpha S_1 + S_2) \cos^3 \gamma \log_e \left( \frac{1 - \sin \gamma}{1 + \sin \gamma} \right) + \\
 & \frac{1}{\pi} (\alpha S_1 + S_2) (1 + \sin^2 \gamma) \cos \gamma \log_e \left( \frac{1 - \cos \gamma}{1 + \cos \gamma} \right)
 \end{aligned}$$

$$\frac{Y}{A_2} = \frac{2\alpha S_1}{\pi} \sqrt{\frac{\sigma_1 - 1}{2}} \tan^{-1} \sqrt{\frac{2}{\sigma_1 - 1}} + \frac{2S_2}{\pi} \sqrt{\frac{\sigma_2 + 1}{2}} \tanh^{-1} \sqrt{\frac{2}{\sigma_2 + 1}} +$$

$$(\alpha S_1 + S_2) \cos \gamma + \frac{1}{\pi} (\alpha S_1 + S_2) (1 + \cos^2 \gamma) \sin \gamma \log_e \left( \frac{1 - \sin \gamma}{1 + \sin \gamma} \right) -$$

$$\frac{1}{\pi} (\alpha S_1 + S_2) \sin^3 \gamma \log_e \left( \frac{1 - \cos \gamma}{1 + \cos \gamma} \right)$$

Using the above results, the functions  $S_1$ ,  $S_2$ , and  $\gamma$  are presented graphically for configurations where

$$\beta = \frac{\pi}{2}$$

and

$$\alpha = 1$$

Figure 5 gives  $S_2$  as a function of  $S_1$  with  $X/A_2$  and  $Y/A_2$  as parameters; figure 6 shows  $S_2$  as a function of  $S_1$  for various values of  $\cos 2\gamma$ . In the  $S_1, S_2$ -plane the entire solution is contained within a distorted diamond-shaped region.

A unique solution is seen to exist for a given physical problem if the hodograph mapping is as shown in figure 2(b). Also, the phenomenon is continuous with respect to  $X/A_2$  and  $Y/A_2$ . Since specific values of  $\alpha$  and  $\beta$  were used in the numerical computation, the curves do not show that the solution is continuous with  $\alpha$  and  $\beta$ . An examination of the original equations, however, does show the steady-state solution to be regular; that is, the phenomenon, as idealized above, is continuous with respect to all of the physical parameters that have been introduced:  $\alpha$ ,  $\beta$ ,  $X/A_2$ , and  $Y/A_2$ . Thus, the assumptions upon which this solution was based do not allow asymmetric flows for a symmetric configuration. Also, for fixed pressures at infinity, it does not seem possible to have the self-excited forces necessary for maintaining an oscillation, although to prove this requires a solution for the nonsteady problem.

For a realistic analysis, therefore, the assumptions of the previous solution must be reexamined and modified. First, if point C is not a stagnation point, multiple solutions are obtained and possible asymmetric flows for a symmetric setup are arrived at. Figure 7(a) shows this flow in the physical plane for  $\beta = \frac{\pi}{2}$ ; the hodograph plane is given in figure 7(b). The  $\zeta$ - and  $\eta$ -planes (see reference 2) are shown in figures 8(a) and 8(b) where

$$\begin{aligned}\zeta &= \log_e iw' \\ &= \frac{1}{2} \log_e \frac{1+s}{1-s} - \log_e \frac{1+2s}{1-2s} \\ s^2 &= \frac{\eta - 0.25}{\eta - 1}\end{aligned}$$

The complex potential  $w(\eta)$  is given by the same expression as in the previous solutions and, as before, the distances X and Y may be determined by integration. It has not been possible to express the integrals in closed form and since the numerical integration is laborious, numerical results for X and Y are not included.

It is clear that for a given geometry there exist at least three solutions:

- (1) One with a stagnation point at C
- (2) One with infinite velocity at C and a stagnation point on AC
- (3) One with infinite velocity at C and a stagnation point on BC

As in the case of two-dimensional flow around airfoils, a Joukowski hypothesis may now be adopted to invalidate those solutions having a point of infinite velocity. If the ducts do not meet at an angle, but are slightly rounded at C, the velocity there is large but finite and at least three solutions may still be expected, namely:

- (1) One with a stagnation point near C
- (2) One with a large velocity at C and a stagnation point on AC
- (3) One with a large velocity at C and a stagnation point on BC

Now the Joukowski hypothesis can no longer be used to eliminate any of the flows and there remains a multiplicity of solutions. This is analogous to the indeterminacy of two-dimensional flow about a rounded body for given conditions at infinity. Although the analysis now gives the possibility of asymmetric flows for symmetric configurations, they are not the kind that are observed; that is, steady-state flows with large velocity in the neighborhood of C are not found experimentally.

A second assumption made for the original solutions is that all of the fluid comes from the same reservoir. Physically, this is the case; in an installation, however, the losses in the two ducts may not be identical and the two streams may arrive at point C with slightly different stagnation pressures. If the stagnation pressures in the two streams are equal at C, the stagnation streamline leaving C bisects the angle  $\beta$ ; but if the two streams have unequal stagnation pressures, point C is a stagnation point in only one stream and the streamline leaves C tangent to one of the ducts. Thus, the flow in the neighborhood of C is unstable with respect to a change in total pressure in one of the ducts; that is, an infinitesimal change in total head of one stream deflects the streamline at C through a finite angle  $\beta/2$ . The character of the flow with unequal stagnation pressures in the two ducts is shown in figure 9; again there are at least three solutions, one with finite velocity everywhere and two with infinite velocity at C. If the line CF is considered fixed at that shape for which both streams have equal total pressures and then if one stagnation pressure is changed infinitesimally, the pressure difference across CF is everywhere infinitesimal. Thus, the instability is confined to the neighborhood of the stagnation point and is not the large-scale kind that is observed experimentally.

A third assumption made for the original analysis is that the ducts discharge into a region of constant pressure. If this assumption is discarded, the phenomenon can be explained in a qualitative way. When it is assumed that the flow leaves the two ducts as a free jet, it is implicitly stated that there is no interaction, neither viscous nor turbulent, between the fluid in the jet and the surrounding fluid in the expanded duct.

It is known, however, that because of turbulent mixing the fluid surrounding a jet is set in motion (reference 3). In the case of a jet discharging into an infinite fluid-filled region, the secondary flow moves laterally toward the jet; that is, adjacent fluid is drawn into the jet and mixes with it. Thus, the jet acts as a pump upon the surrounding fluid. Because of the pumping action there is a region of low pressure at either side of the jet. This is also true if the jet discharges into an expanded duct instead of into an infinite space, the low-pressure region becoming more pronounced as the duct width decreases.

Thus, the forces that arise because of turbulent mixing favor instability of the jet; for example, with a symmetric setup, if the jet is displaced slightly to the left of the line of symmetry, the pressure between the jet and the left duct wall will decrease and tend to aggravate the asymmetry.

To determine whether a particular state is stable or not, the relative influence of mixing and the stabilizing effects due to symmetry of geometry and boundary conditions must be investigated. As shown in the next section, under certain conditions the turbulent mixing effect dominates and the jet swings over toward one duct wall and is stable there; under other conditions a balance is achieved between the mixing and symmetry effects allowing the jet to oscillate laterally about the symmetry position.

Since there is no straightforward and reliable method for solving the flow problem including the turbulent-mixing phenomenon, a potential solution that has some of the essential characteristics of the turbulence problem would be of interest. As seen from typical observed flow patterns in figure 10, the mean streamlines in the secondary flow are closed curves. This has suggested the consideration of a potential solution for a flow discharging into an expanded duct where there are appropriate vortex singularities between the jet and the duct walls. It is anticipated that such an analysis would allow a quantitative study of the jet stability.

#### EXPERIMENTAL ANALYSIS

Since the theoretical analysis was carried out for the two-dimensional problem, the apparatus for the experimental analysis was constructed on a two-dimensional basis. Water was used in the experiments for the following reasons:

- (1) The flow could be made visible through the use of dyes
- (2) Instrumenting the apparatus for water would be relatively simple
- (3) A large 25-foot-high and 5-foot-diameter reservoir which could be used as a steadyng tank for the fluid was available in the laboratory
- (4) Water would allow a comparison between the stability of a free jet and one issuing into a region of comparable density

The purpose of the first experiments was to simulate the simplified conditions assumed in the first theoretical analysis; that is, to study the stability of a free jet discharging out of two converging ducts. For this purpose a simple water table was used. It consisted of two 6- by 3-foot sheets of plate glass  $\frac{1}{4}$  inch thick forming the top and bottom planes separated by strips of copper 1 inch high and  $\frac{1}{4}$  inch thick arranged so as to form two rectangular reservoir sections, each with one duct outlet. The two ducts, which converged at an angle of  $15^\circ$ , were each  $\frac{1}{2}$  inch wide, and emptied into the atmosphere between the two glass plates (fig. 11).

Water from the pressurized tank passed through throttling valves which allowed a difference in stagnation pressures to be maintained in the two reservoir sections. Thus, the jet could be made to swing through an angle of  $7\frac{1}{2}^\circ$  to each side of the line of symmetry. The use of copper and glass components, however, made it difficult to achieve both watertight seals and the desired flexibility in geometry.

In addition, a second model of two ducts discharging into a simple expanded duct was constructed. This, again, was two-dimensional with two 6- by 3-foot sheets of Lucite  $\frac{1}{4}$  inch thick as upper and lower surfaces. The reservoir and the two ducts were formed of 1-inch-square bars of Lucite. The ducts, which converged at an angle of  $15^\circ$  and were  $\frac{1}{2}$  inch wide, led into a rectangular sink section that discharged through an aperture of variable area (figs. 12 and 13). The reservoir was not divided in this case. All sections were instrumented to allow pressure measurements and dye insertion.

The system was sealed by bolting the top and bottom sheets to the duct, reservoir, and sink components. A thin layer of glazing compound between contacting surfaces was used to compensate for slight irregularities. Provisions were made for varying both the side walls of the sink and exit aperture. However, the reservoir, duct length, duct convergence angle, and length of the sink were kept constant during all tests.

Model I was used to investigate the stability of the jet in symmetric and asymmetric positions, asymmetric flows being due to a difference in reservoir pressures. The experiments were conducted over a range of mass flows from 0.005 to 0.050 cubic foot per second. It was necessary to insert dye into one reservoir in order to obtain clear photographic records. Figure 14 shows a typical free jet emerging from the two ducts with equal reservoir pressures. The jet was found to be stable in all possible symmetric and asymmetric positions, and, also, the configurations were found to be unique for given reservoir conditions. Oscillations of the jet, artificially excited by short-duration

fluctuations in reservoir pressures, were found to damp out rapidly upon removal of the disturbing forces; that is, it was not possible to induce self-excited oscillations. These results are in agreement with the free-jet potential solution which satisfies a Joukowski hypothesis.

The experiments using model II were run for a variety of configurations to study the stability of a jet of water discharging into an atmosphere of water. As in model I, the fluid entered the system through two slit tubes located at the head of the reservoir section. The range of mass flow covered is listed below:

(1) When the two converging ducts discharging into the expanded duct (or sink) had a width of  $27\frac{1}{2}$  inches, an aperture of diameter

$d = 1$  inch produced a flow of 0.024 to 0.065 cubic foot per second; when  $d = 2$  inches, a flow of 0.031 to 0.095 cubic foot per second was produced.

(2) When the duct width was 18 inches (A-A in fig. 12),  $d = 1$  inch produced a flow of 0.027 to 0.058 cubic foot per second,  $d = 2$  inches produced a flow of 0.026 to 0.039 cubic foot per second, and  $d = 3$  inches produced a flow of 0.032 to 0.090 cubic foot per second.

(3) When the duct width was 14 inches (B-B in fig. 12),  $d = 1$  inch produced a flow of 0.020 to 0.065 cubic foot per second,  $d = 2$  inches produced a flow of 0.020 to 0.083 cubic foot per second, and  $d = 3$  inches produced a flow of 0.027 to 0.093 cubic foot per second.

(4) When the duct width was 10 inches (C-C in fig. 12),  $d = 1$  inch produced a flow of 0.014 to 0.061 cubic foot per second,  $d = 2$  inches produced a flow of 0.025 to 0.090 cubic foot per second, and  $d = 3$  inches produced a flow of 0.020 to 0.089 cubic foot per second.

(5) When the duct width was 6 inches (D-D in fig. 12),  $d = 1$  inch produced a flow of 0.019 to 0.071 cubic foot per second,  $d = 2$  inches produced a flow of 0.020 to 0.093 cubic foot per second, and  $d = 3$  inches produced a flow of 0.028 to 0.097 cubic foot per second.

(6) When the sink walls were flush with the two converging ducts at a width of  $1\frac{1}{64}$  inches, an aperture opening equal to the sink separation produced a flow of 0.020 to 0.089 cubic foot per second.

The flow was made visible by inserting dye into the sink through pressure taps  $P_3$  and  $P_6$  or  $P_4$  and  $P_5$ . Figure 15 is a photograph of a jet of clear water issuing into the sink. With model II three different

kinds of flows were observed. The first was unsteady with the jet oscillating laterally about the line of symmetry, the motion being stable with respect to external disturbances. This was found at a sink width of  $27\frac{1}{2}$  inches. For the 1-inch aperture, the oscillations were periodic with random fluctuations superimposed. For the 2-inch aperture, the oscillations were small and showed no definite period. No data were taken for the 3-inch aperture since the sink could not be kept filled with water. Figure 10(a) shows the vortex configuration of the fluid in the sink for both the 1- and 2-inch apertures.

The second kind of flow was observed at a sink width of 18 inches for 1-, 2-, and 3-inch apertures. In this case, the jet was able to assume any one of three configurations for a given setting; the jet either oscillated about the line of symmetry with a definite frequency or it was steady in an asymmetric position deflected toward one of the sink walls. All three flows, the oscillatory and the two asymmetric ones, were stable with respect to small disturbances; that is, once the jet was in a given state, it remained there indefinitely, even when subjected to small, external perturbations. When the flow was exposed to sufficiently large disturbances, however, it was possible to move the jet from one state to either of the other two. The irregularities in the flow under normal operating conditions were too small to cause a jump from one configuration to another. External disturbances were produced in several ways. One method was to insert a rod into the sink through the aperture and then to move the rod rapidly away from one of the sink walls. This created a low-pressure region near that wall which drew the jet into an asymmetric position from either the oscillatory state or the opposite asymmetric position. Another means of disturbing the flow was to inject water for a short time into the sink through pressure taps  $P_3$ ,  $P_4$ ,  $P_5$ , or  $P_6$  (see fig. 12). Injecting water through  $P_6$  at a velocity comparable with the jet velocity aided the pumping action of the jet upon the fluid near the right-hand sink wall. Thus, the pressure near that wall decreased and the jet moved from either of the other two positions into the asymmetric state to the right of the symmetry axis. If the jet were asymmetric to the right, injecting water through  $P_5$  counteracted the pumping effect of the jet near the right wall and relieved the low-pressure region there. This caused the jet to assume the oscillatory state or the opposite asymmetric position. Similar results were found for  $P_3$  and  $P_4$ . Figure 15 is a photograph of the jet in a steady, asymmetric flow. Figure 10(b) shows the vortex configuration in the sink with the jet oscillating about the axis of symmetry. A typical vortex configuration for an asymmetric flow is given in figure 10(c).

The third kind of flow that occurred in model II was steady with the jet asymmetric to the left or right. This was observed at sink widths of 14, 10, and 6 inches with 1-, 2-, and 3-inch apertures. With

care, it was possible to obtain a symmetric flow for a few seconds; the configuration, however, was unstable and very quickly changed to a stable, asymmetric pattern such as shown in figure 10(c). Sufficiently large external disturbances, such as described in the previous case, could change the flow pattern from one stable configuration to the other.

Several tests were also carried out with the sink walls flush with the converging ducts, and these tests did not represent the flow out of two ducts into an expanded duct. For these conditions, no oscillations or asymmetries were observed; the jet simply filled the sink.

Figures 16 and 17 summarize the important results of the experiments with model II. Figure 16 is a stability diagram in the mass-flow sink-width plane showing three regions: Stable oscillatory symmetric flows for large sink widths, stable oscillatory or asymmetric flows for intermediate sink widths, and stable asymmetric flows for small sink widths. The separating lines between these regions were inferred from test data and were not determined precisely from experiments. Since the kinds of flows that were observed appeared to be independent of the aperture widths, the latter does not appear as a variable in figure 16. Lack of time prevented a more comprehensive survey. Curves of mass flow against frequency are shown in figure 17. It is seen that the frequency of oscillation increases with mass flow for a given geometry. Also, for a given sink width and constant mass flow the frequency increases with increasing aperture. The curves indicate that for a given aperture and a constant mass flow, an increase in sink width causes an increase in frequency.

Harvard University  
Cambridge, Mass., December 29, 1949

#### REFERENCES

1. Milne-Thomson, L. M.: *Theoretical Hydrodynamics*. Macmillan and Co., Ltd. (London), 1938, p. 283.
2. Churchill, Ruel V.: *Complex Variables and Applications*. McGraw-Hill Book Co., Inc., 1948, p. 181.
3. Tollmien, Walter: *Berechnung turbulenter Ausbreitungsvorgänge*. Z.f.a.M.M., Bd. 6, Heft 6, Dec. 1926, pp. 468-478. (Also issued as NACA TM 1085, 1945.)

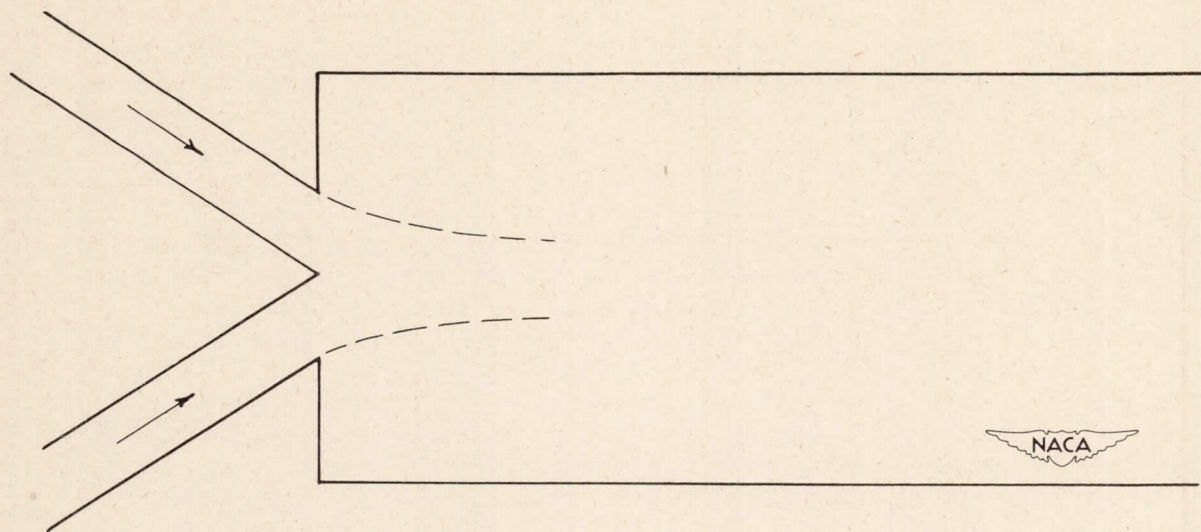
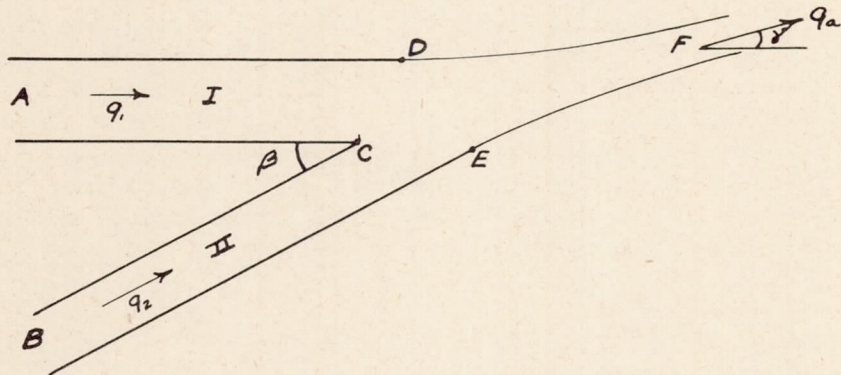
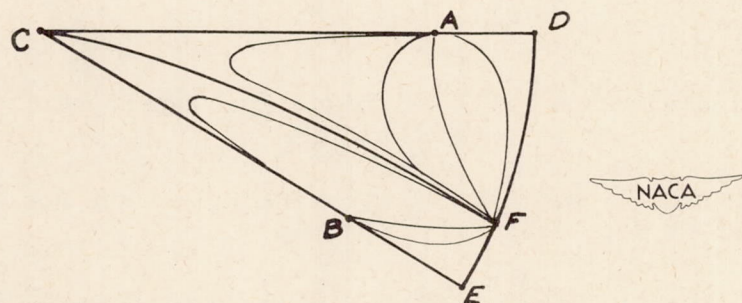


Figure 1.- Two ducts discharging into a single duct.



(a) Physical  $z$ -plane.



(b) Hodograph  $w'$ -plane.

Figure 2.- Physical and hodograph planes for two streams converging at an angle  $\beta$ .

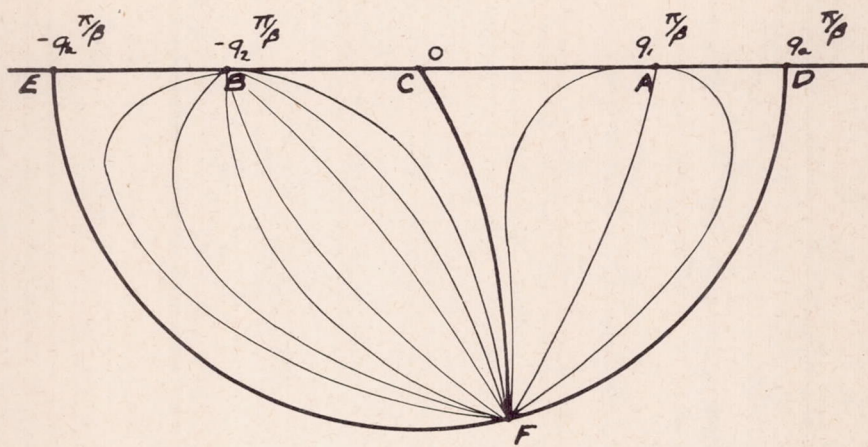
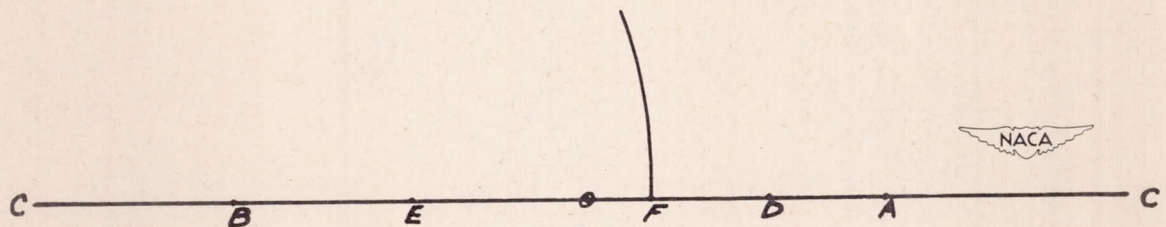
(a)  $\zeta$ -plane.(b)  $\eta$ -plane

Figure 3.-  $\zeta$ - and  $\eta$ -planes for two streams converging at an angle  $\beta$ .

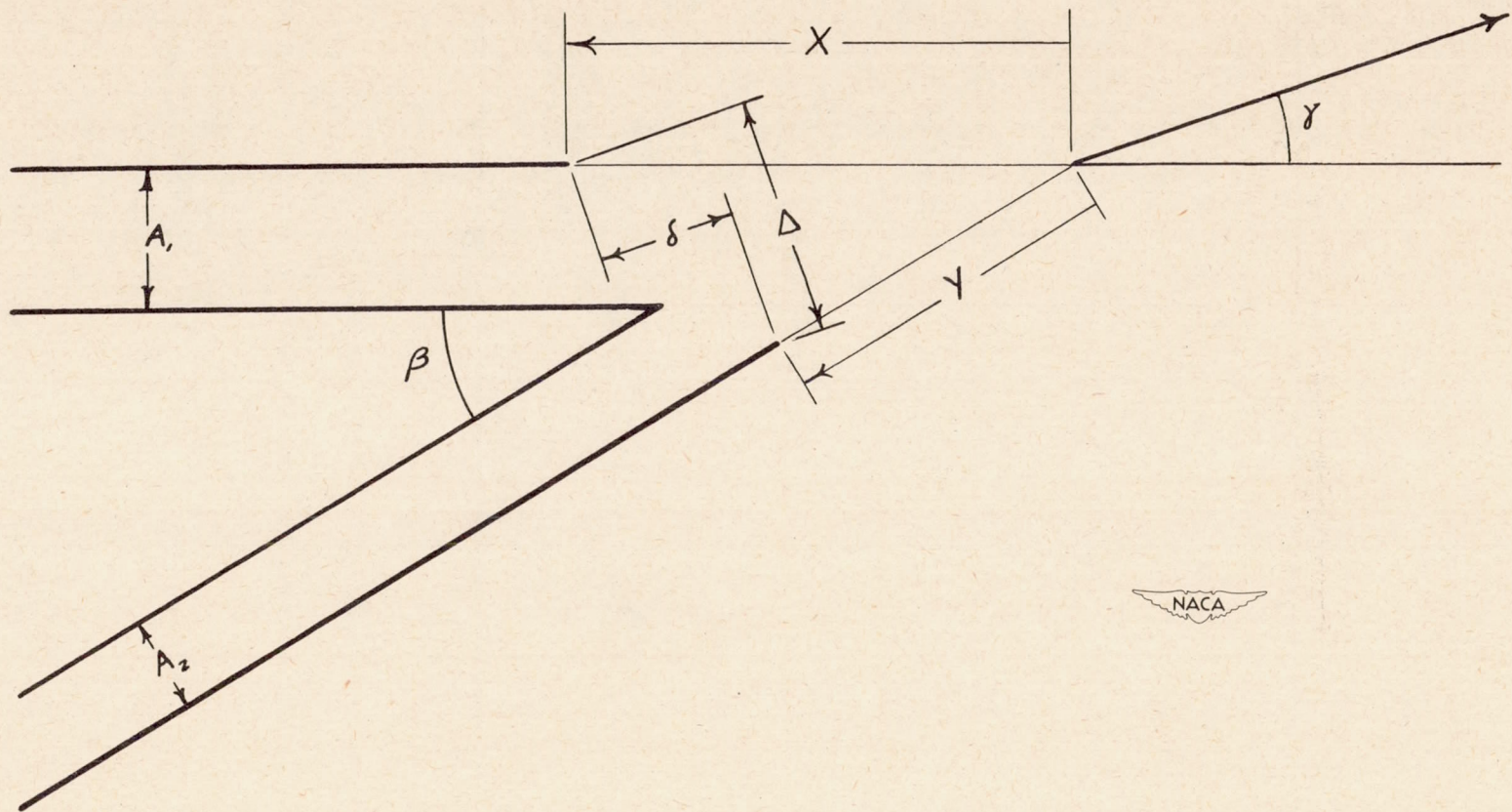


Figure 4.- Physical plane, with dimensions, for two converging streams.

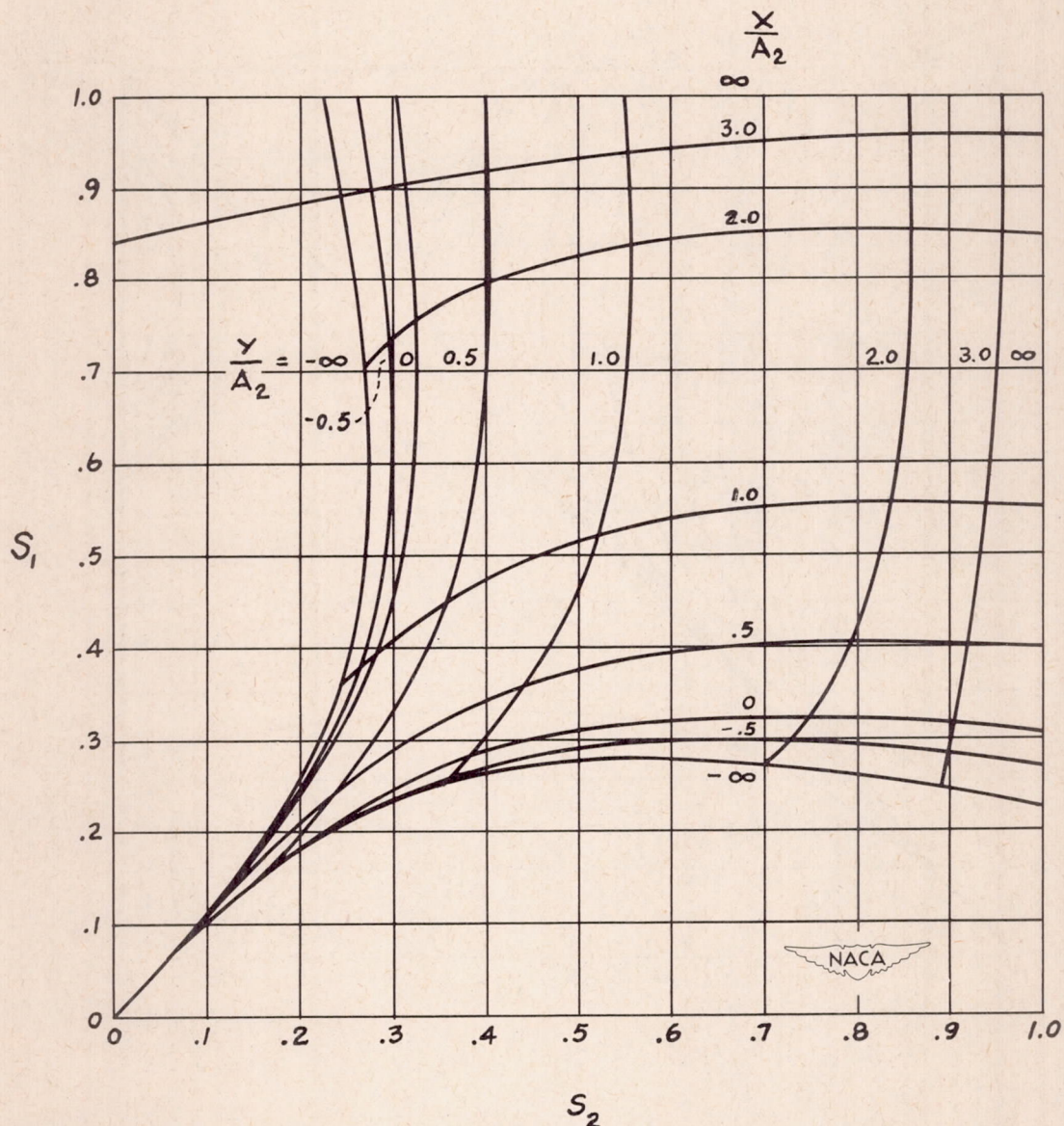


Figure 5.- Curves of  $S_1$  against  $S_2$  for various values of  $X/A_2$  and  $Y/A_2$ .

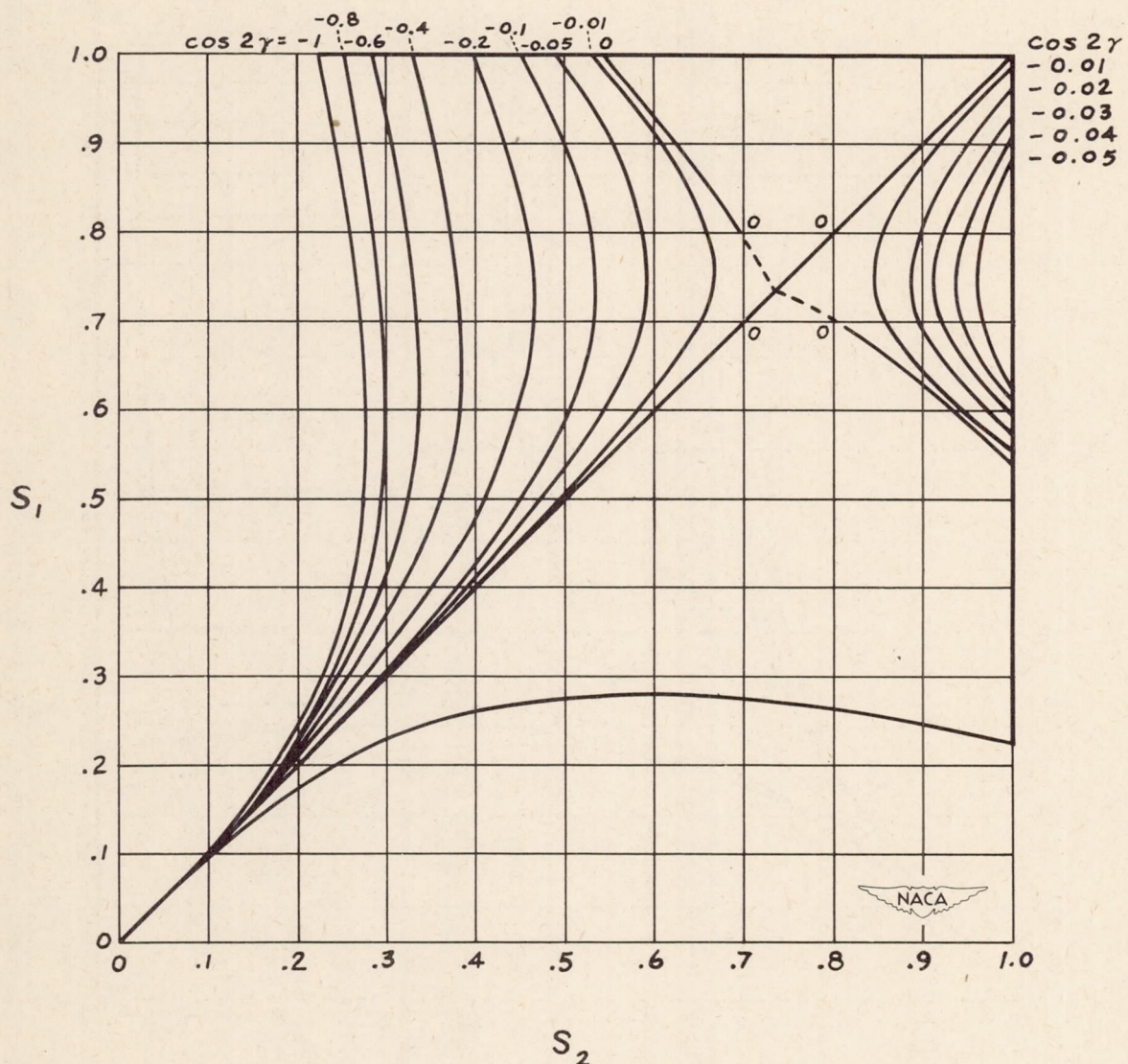


Figure 6.- Curves of  $S_1$  against  $S_2$  for various values of  $\cos 2\gamma$ .  
For positive values of  $\cos 2\gamma$ , reflect given curves about diagonal.

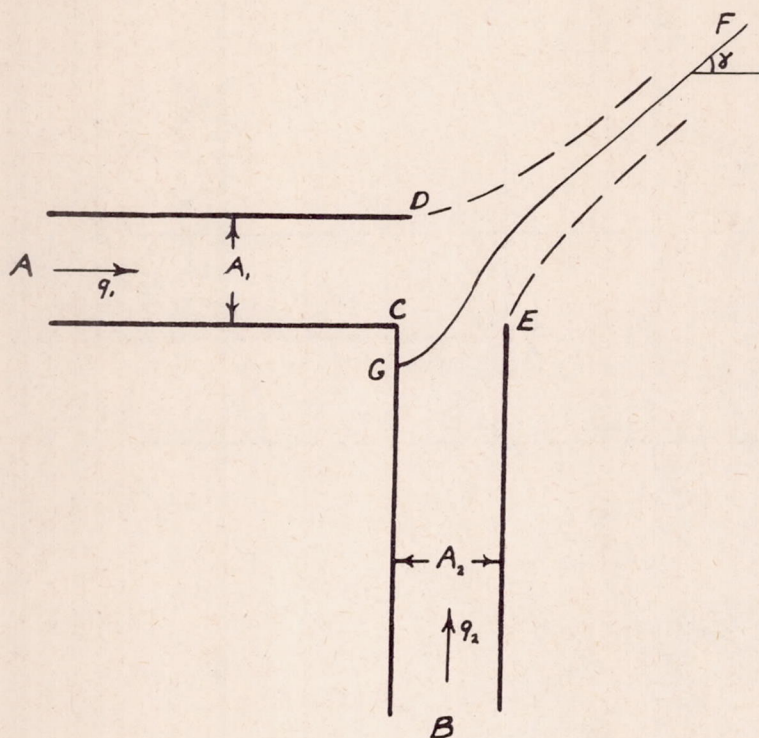
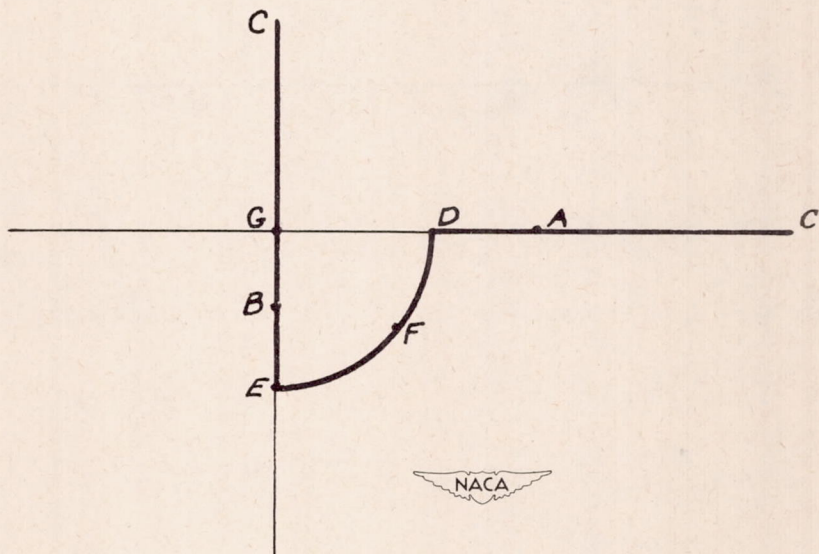
(a) Physical  $z$ -plane.(b) Hodograph  $w'$ -plane.

Figure 7.- Physical and hodograph planes for two streams converging at right angles.

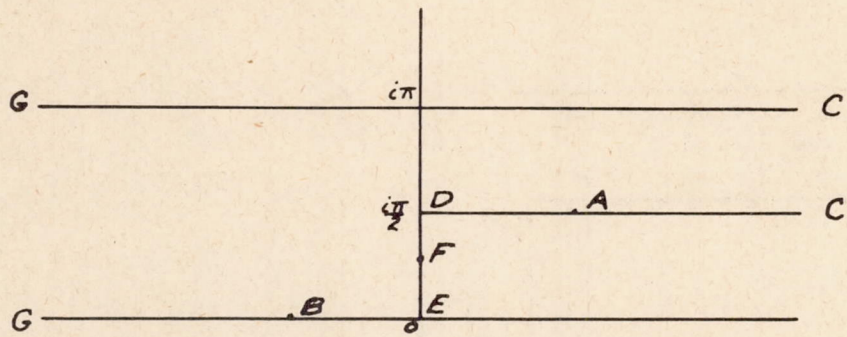
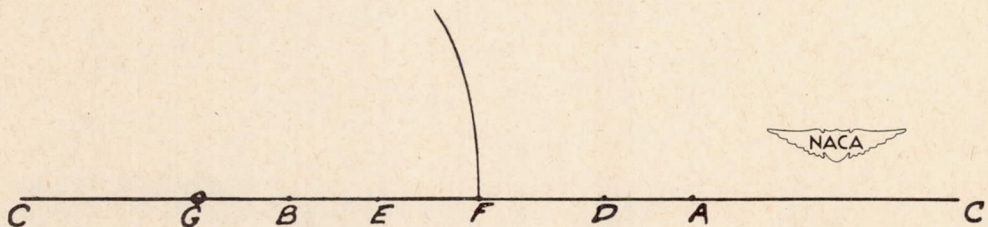
(a)  $\zeta$ -plane.(b)  $\eta$ -plane

Figure 8.-  $\zeta$ - and  $\eta$ -planes for two streams converging at right angles.

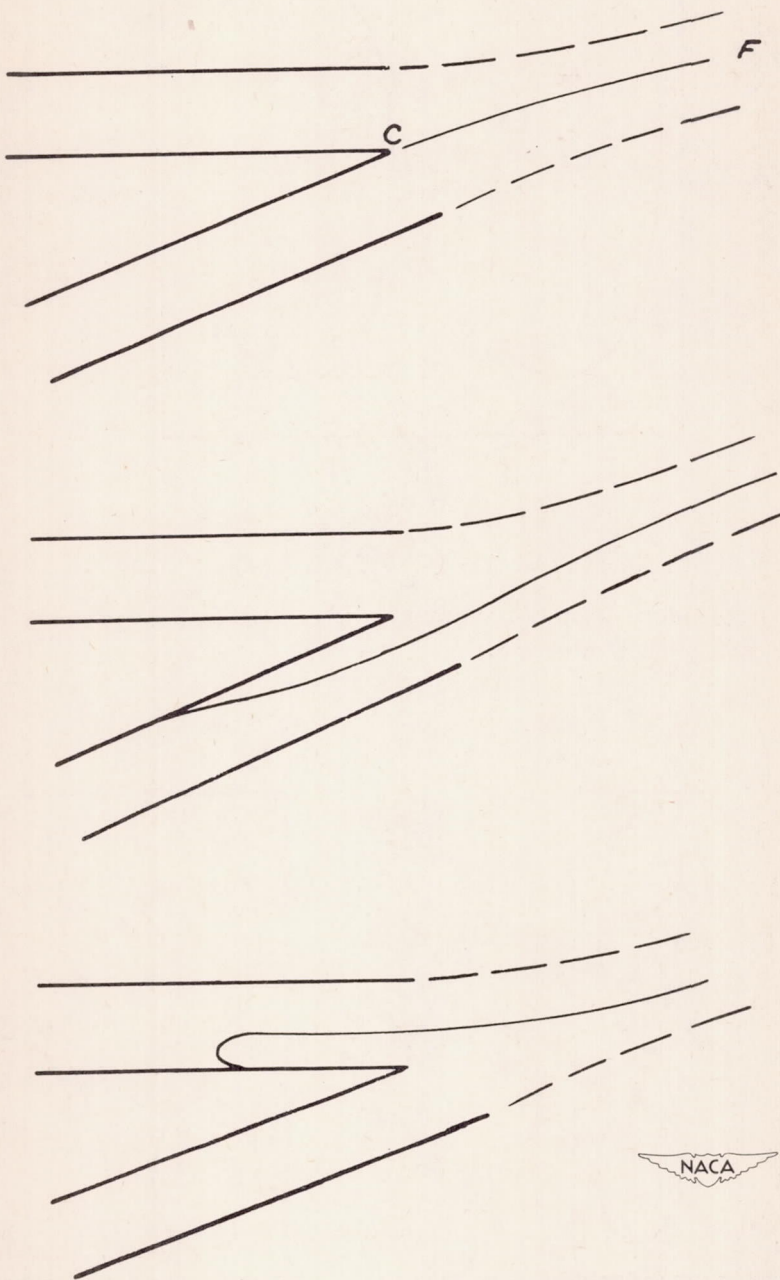
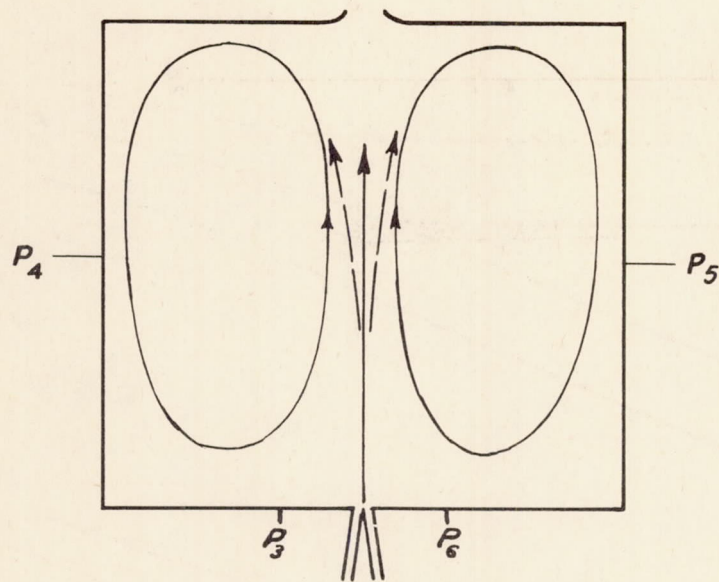
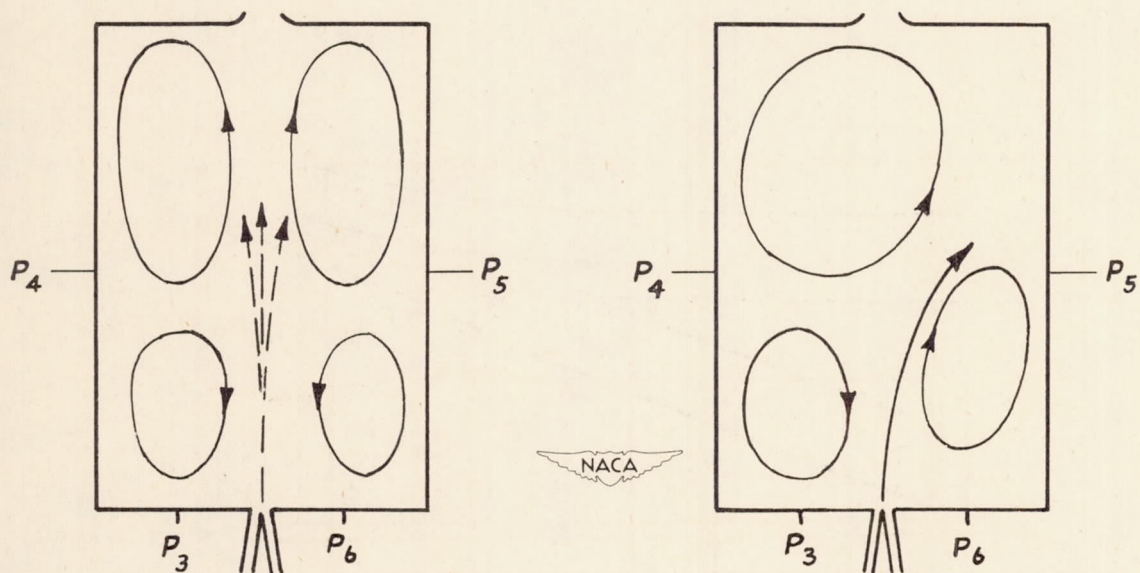


Figure 9.- Typical flow patterns caused by unequal stagnation pressures in ducts.



(a) Configuration in  $27\frac{1}{2}$ -inch sink. Flow is unsteady with jet oscillating laterally about axis of symmetry.



(b) Configuration with 18-inch sink.  
Jet is oscillating about axis of symmetry.

(c) Configuration with 14-, 10-, or 6-inch sink. Flow is stable with jet asymmetric.

Figure 10.- Typical vortex configurations observed in experimental analysis.

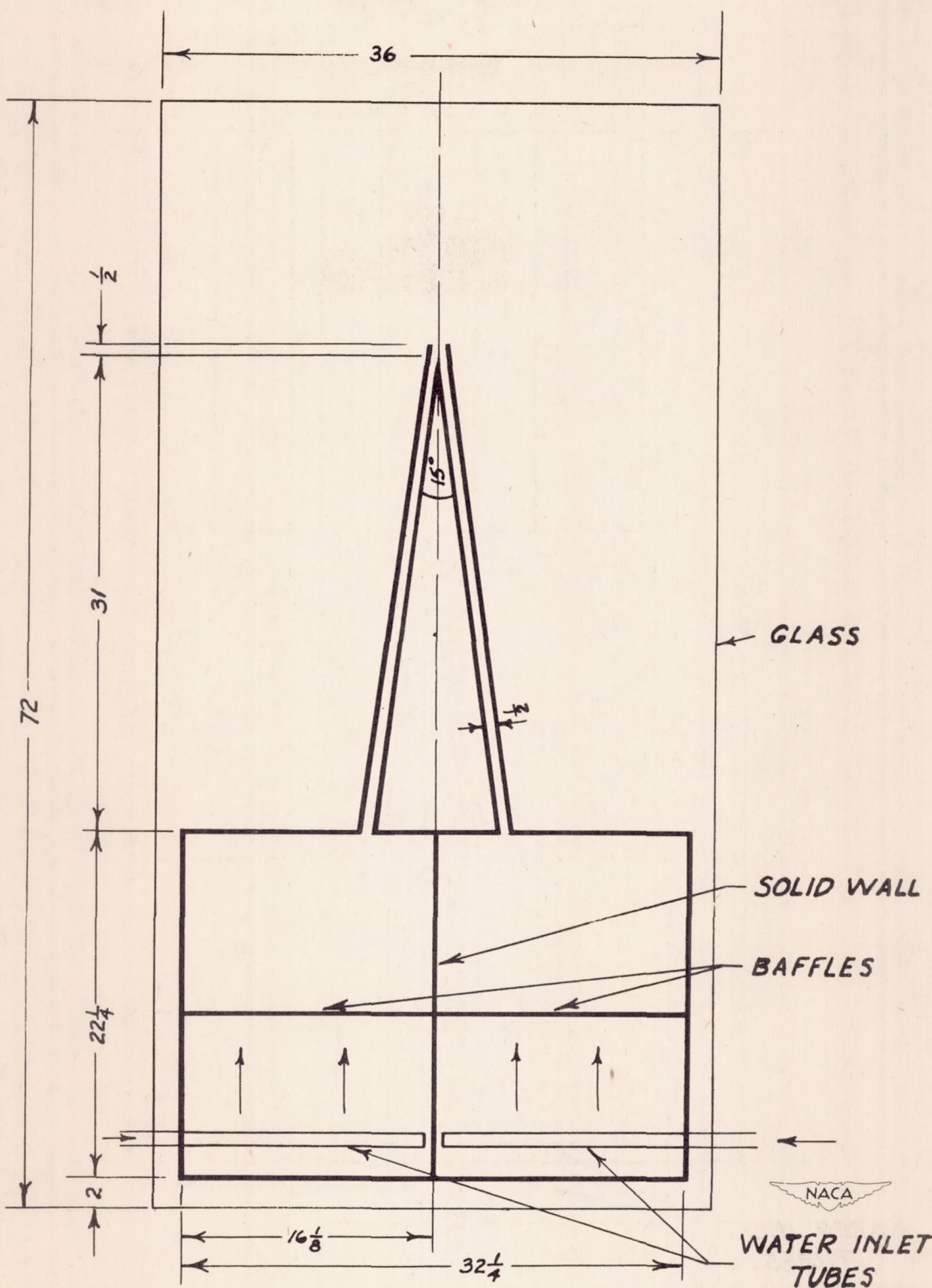


Figure 11.- Water table I. Dimensions are in inches.

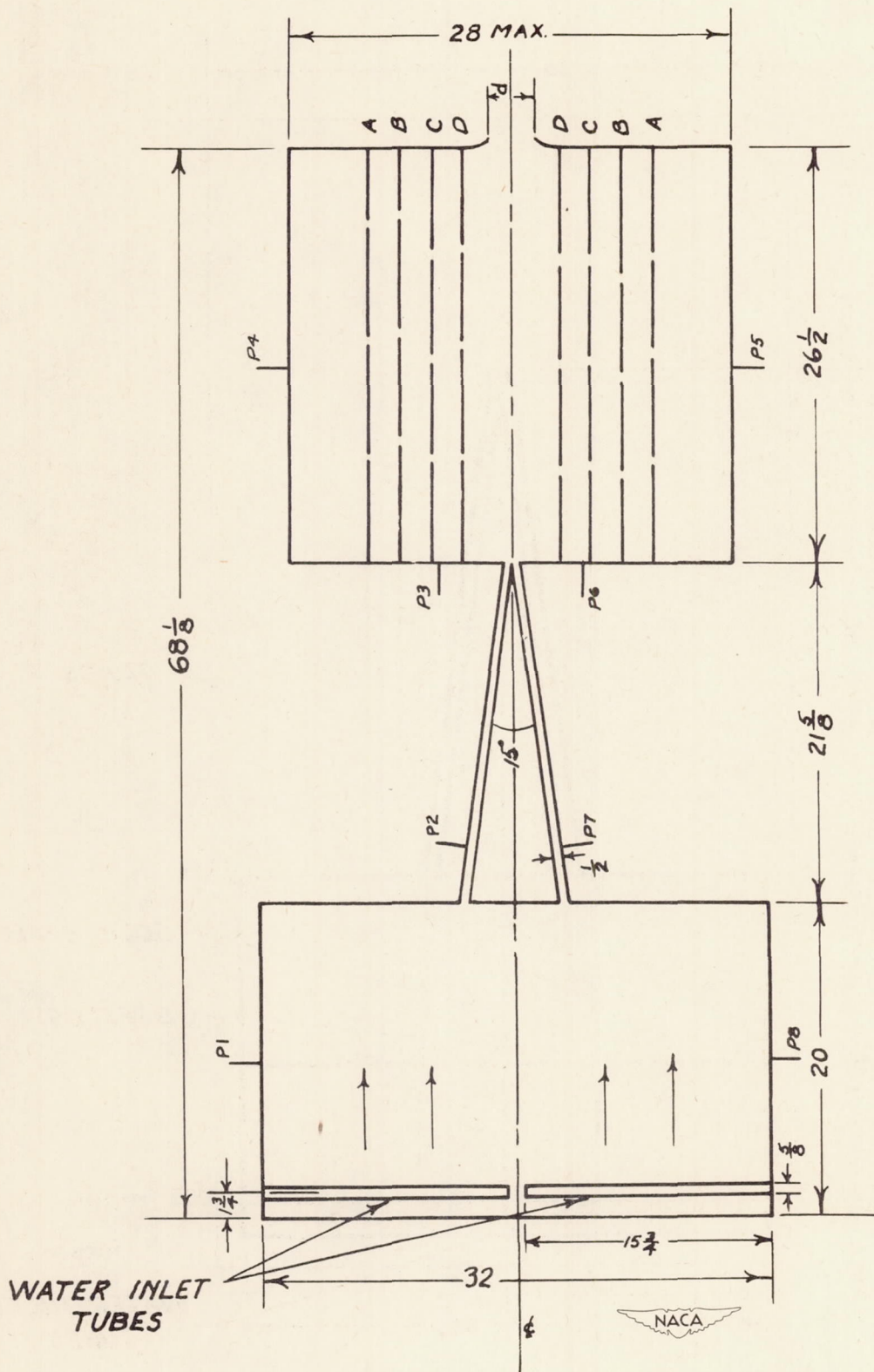


Figure 12.- Water table II. Dimensions are in inches.

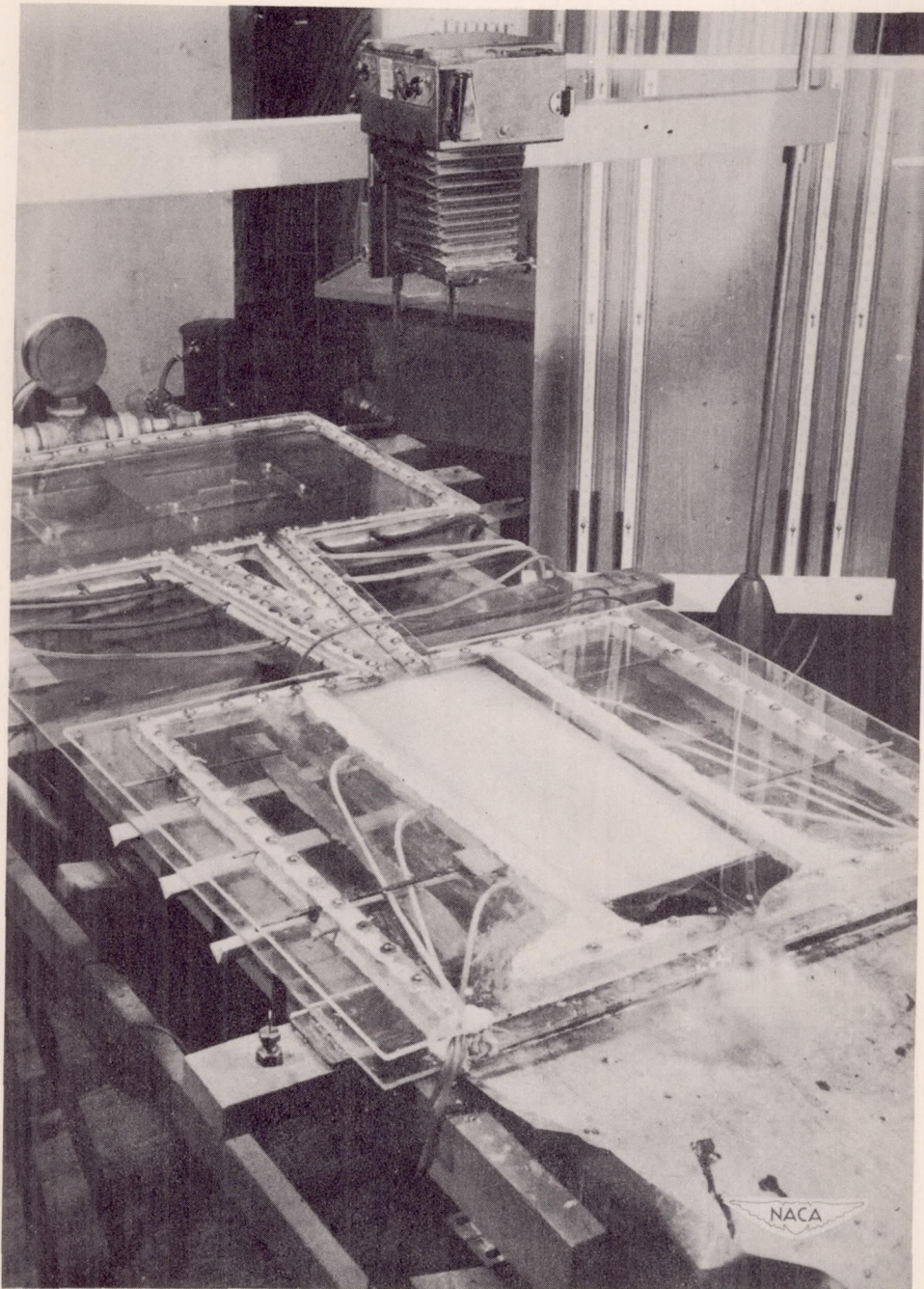


Figure 13.- Test setup.

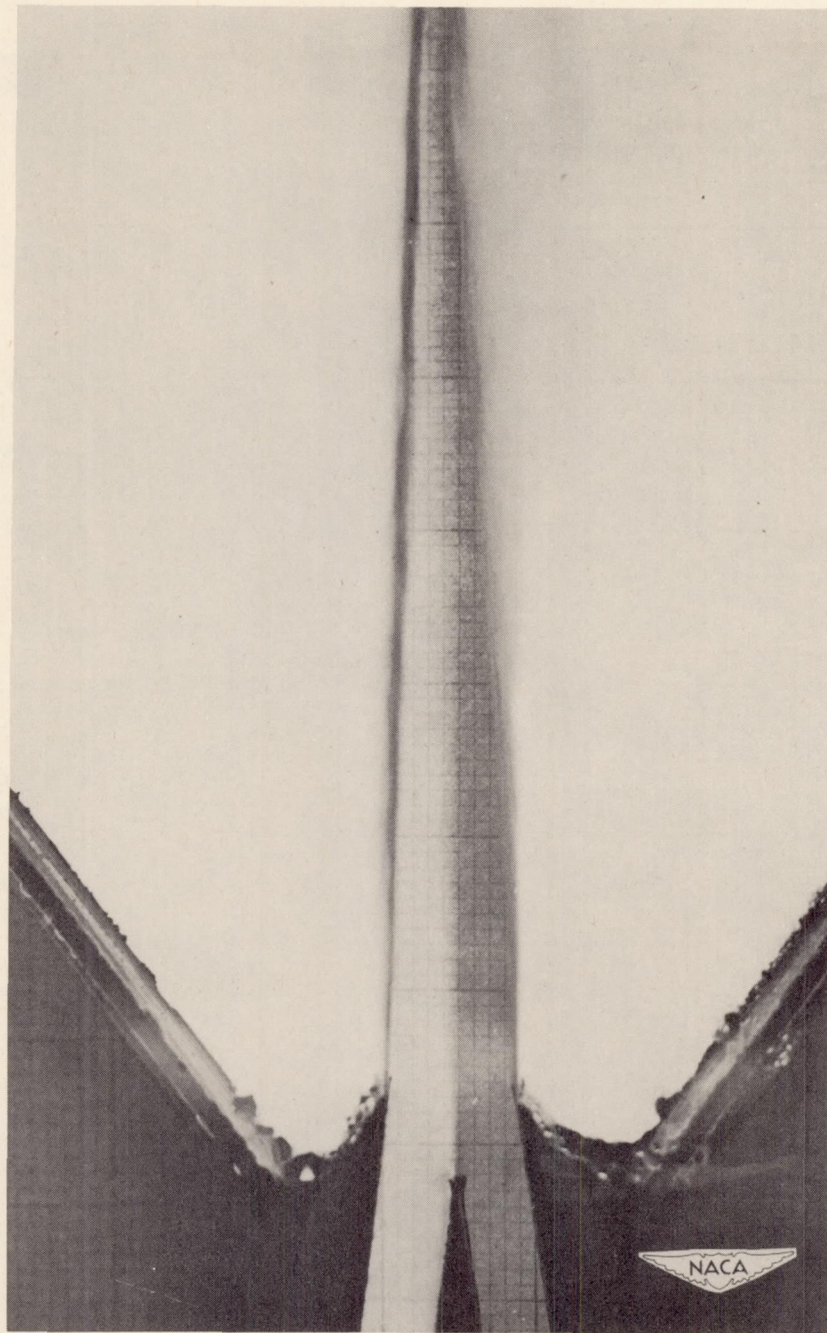


Figure 14.- Typical free jet emerging from two ducts with equal reservoir pressures.

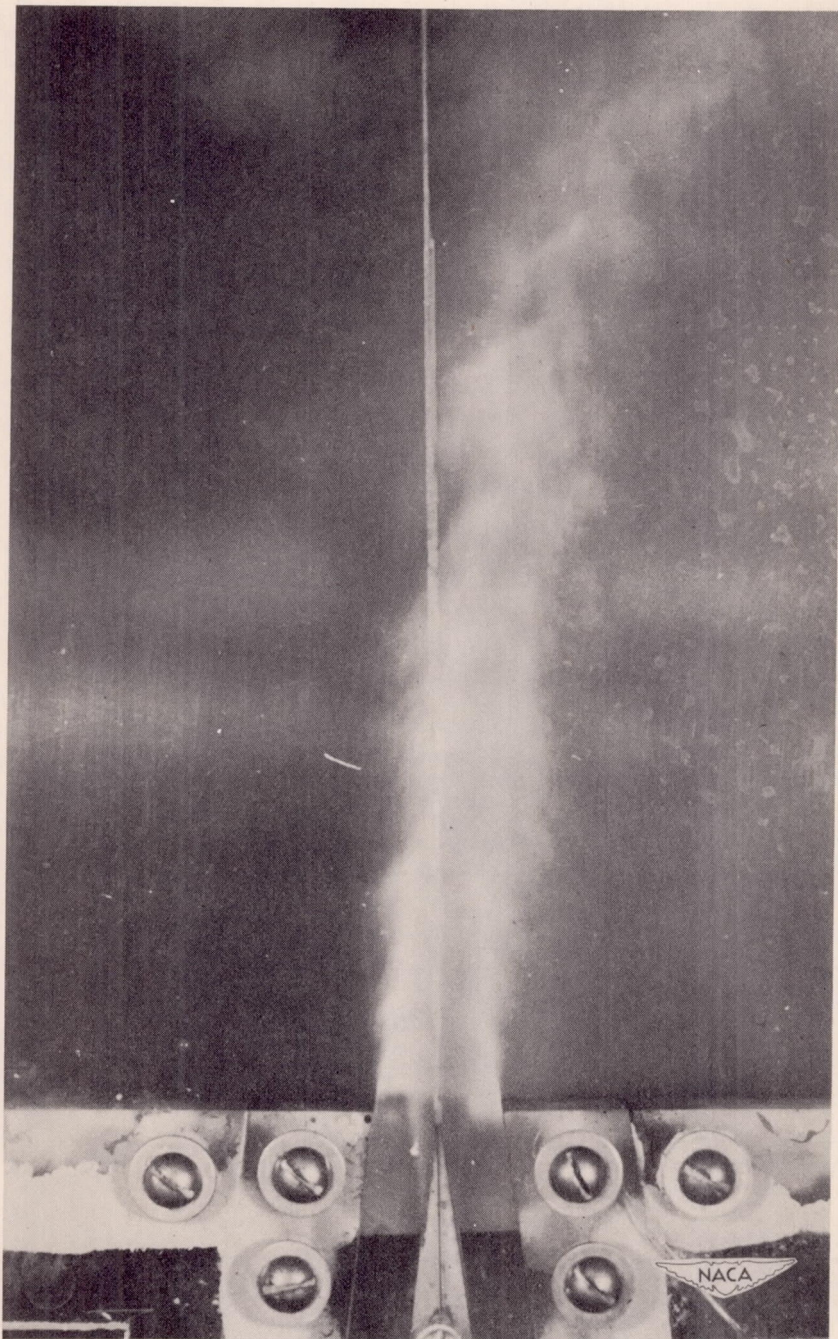


Figure 15.- Jet of clear water issuing into sink.

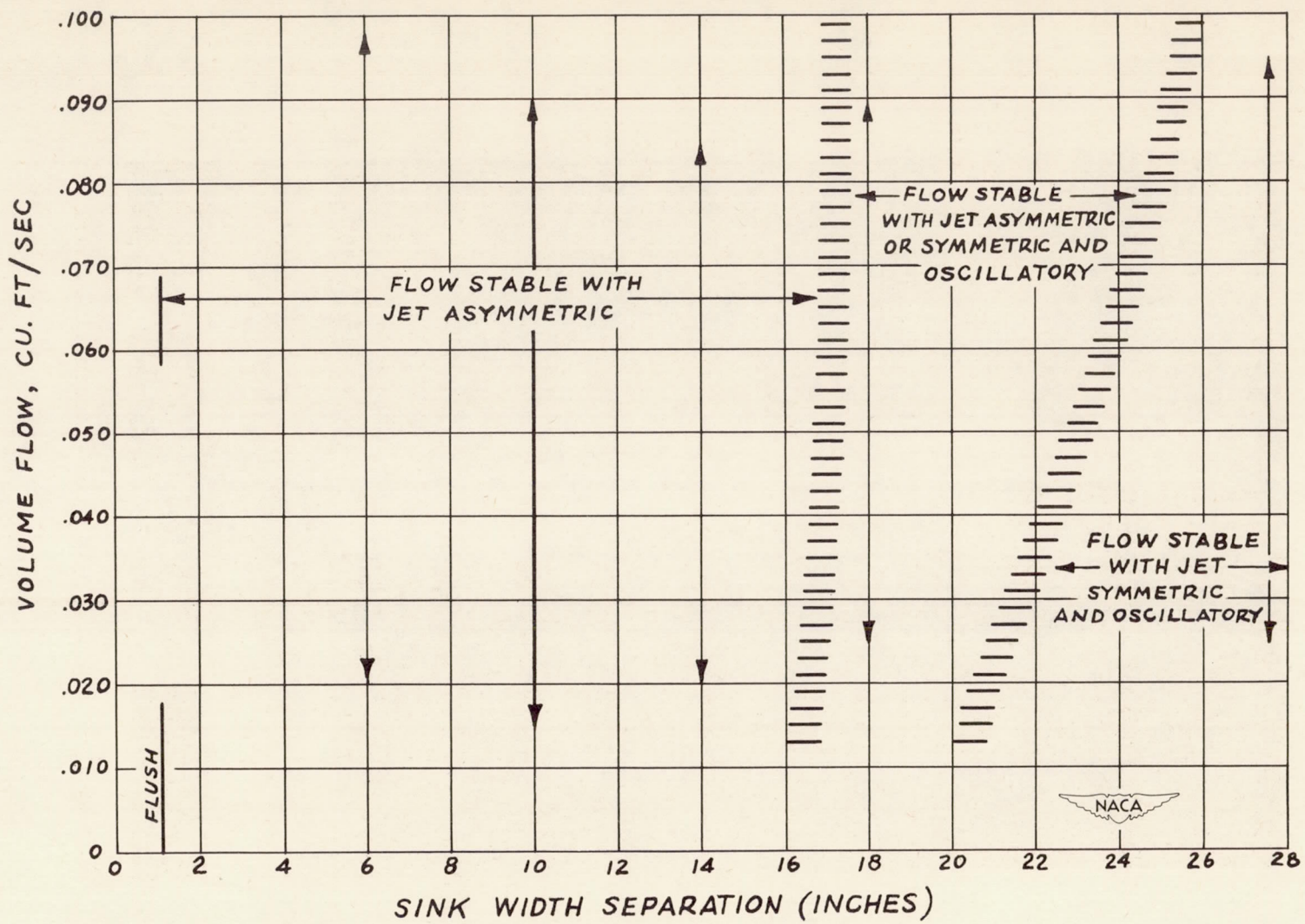


Figure 16.- Stability diagram. Vertical lines indicate range of volume flow.

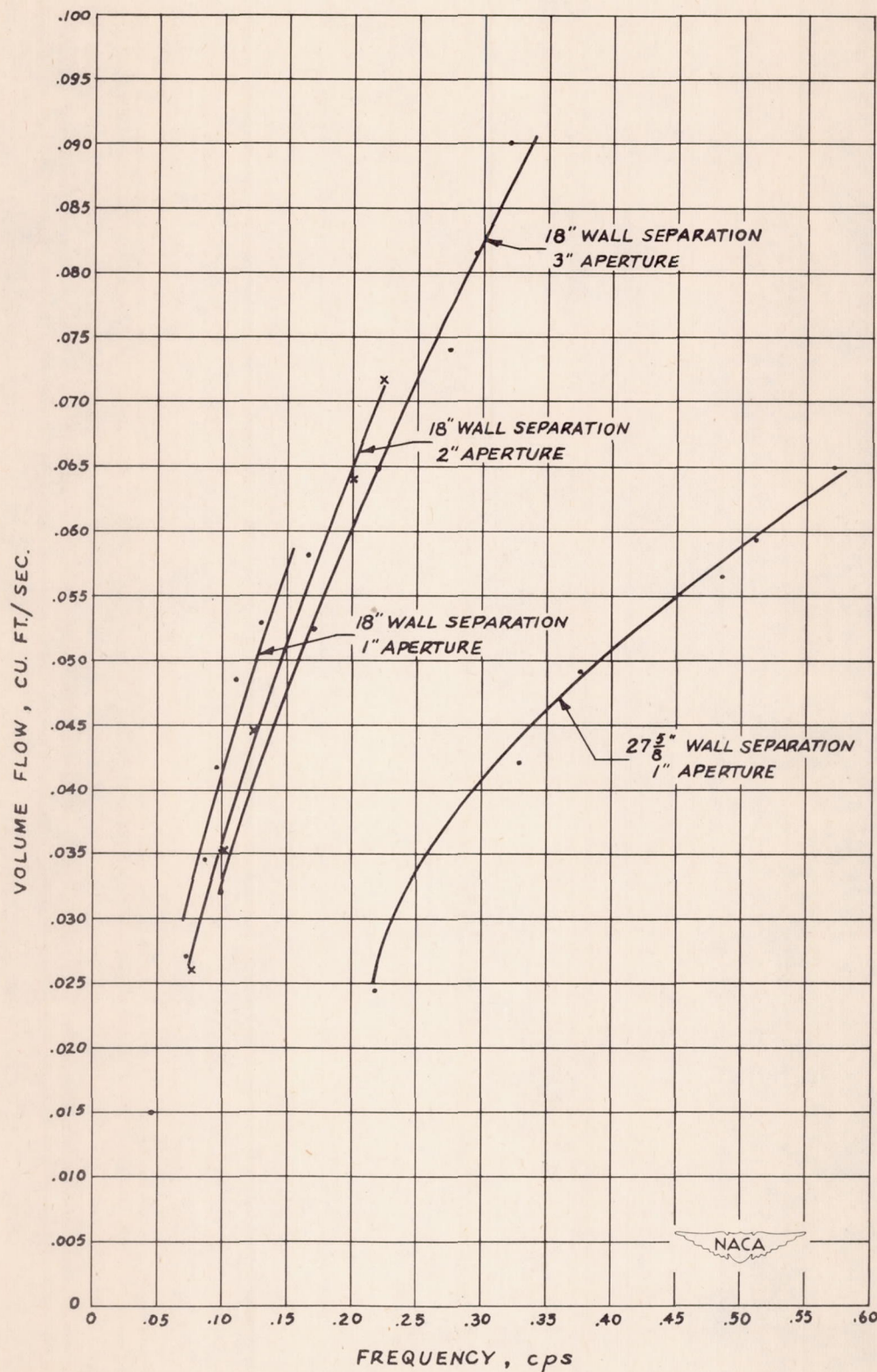


Figure 17.- Curves of mass flow against frequency. Sink walls and aperture are symmetric.